**U.S. DEPARTMENT OF THE INTERIOR**

**U.S. GEOLOGICAL SURVEY**

# AEROMAGNETIC AND GRAVITY STUDIES OF PAYETTE NATIONAL FOREST, IDAHO

**By**

**M. Dean Kleinkopf**

Open-File Report 98-219 D

1998

## CONTENTS



## ILLUSTRATIONS



## TABLE

## ABSTRACT

Aeromagnetic and gravity anomaly maps were compiled and interpreted to help define buried structure and igneous intrusions that might influence localization of undiscovered mineral deposits of the Payette National Forest. Three geologic terranes span the forest and exhibit distinctive aeromagnetic signatures. The Idaho batholith granitic terrane along the western edge of the North American continental craton exhibits a flat featureless field, except for pronounced highs associated with diorite and tonalite intrusive rocks along the western edge, 2) the terrane of the Salmon River suture zone reflects distinctive linear magnetic highs over mafic intrusions common in the zone and, 3) the allochthonous island-arc terrane of oceanic origin, consisting of metamorphosed plutonic, and volcanogenic, clastic, and carbonate rocks, coupled with effects of high magnetic susceptibility Columbia River basalts, resulted in numerous discrete aeromagnetic highs and lows with sources that are often fault controlled.

Granitic rocks of the Tertiary (Eocene) epizonal plutons, located in the eastern part of the forest, were observed to have a higher magnetic susceptibility ($180 \times 10^{-5}$ cgs units) than granodiorite and two-mica granite rocks of the Cretaceous Idaho batholith interior ($50 \times 10^{-5}$ cgs units). Residual aeromagnetic anomaly maps, in shaded relief, were prepared by wave-length filtering (50 km high pass) the total-intensity data that had been reduced-to-the-pole. Pseudogravity gradient maxima were plotted on the map to help delineate magnetization boundaries that might signify geologic contacts or linear geologic features, such as faults or dikes.

To supplement the aeromagnetic interpretations, a high pass isostatic residual gravity anomaly map was prepared to help distinguish subtle anomalies due to local sources in the upper part of the crust. The gravity anomaly data, in some cases, provided constraints on the interpretations of the aeromagnetic anomaly data and the geology, in applications to the mineral resource assessment. In particular, low amplitude gravity lows were observed to result from subtle density differences between most of the Cretaceous ( 2.60 $g/cm^3$) and Tertiary granites (2.57 $g/cm^3$).

The USGS Payette Forest minerals assessment team prepared permissive tract maps of mineral resource deposit models that might be expected to occur in Payette National Forest. To demonstrate applications of aeromagnetic anomaly data in the assessment process, permissive tracts for four of the mineral deposit models are plotted on the residual aeromagnetic anomaly map of the forest.

## INTRODUCTION

Aeromagnetic and gravity anomaly patterns reflect granitic, volcanic, and metamorphic terranes that shape the landscape and host metallic and industrial mineral resources in the Payette National Forest (PNF). This study was part of a multi-disciplinary assessment of undiscovered mineral resources of the forest by a team of earth scientists in the Mineral Resource Program of the U.S. Geological Survey (USGS). The purpose was to compile and interpret aeromagnetic and gravity anomaly maps and define buried structure and igneous intrusions that might influence localization of mineral deposits. The maps are companion maps to mineral deposit, geological, geochemical, and radioelement maps that are in preparation for separate reports by other members of the Payette team (Bookstrom and others, in prep., 1998; Lund and others, 1998; Pitkin, in prep., 1998; Watts and King, in prep., 1998).

Aeromagnetic and gravity anomalies result from juxtaposition of rocks of contrasting physical properties. The aeromagnetic anomaly data distinguish highly magnetic mafic rocks such as basalts, from weakly-moderately magnetic rocks, such as granites, hydrothermally altered rocks, and most sedimentary rocks. Aeromagnetic anomaly patterns generally provided more detail about shallow structure and lithology than the gravity anomaly data because of the greater volume of data collected along aeromagnetic profiles in contrast to the 3-4 km randomly spaced gravity observations. In addition, the greater range of values of magnetic properties compared with the smaller range of density values of most rocks provided more detail in discriminating individual lithologies. Aeromagnetic anomaly data used in detailed exploration studies may exhibit signatures of geologic features that have associated mineral deposits, therefore providing information for identification of other areas possibly favorable for the occurrence of similar deposits. The gravity anomaly data help identify large lithologic units and major fault zones on the basis of density contrasts resulting from juxtaposition of rocks of different density. For example, gravity lows may reflect granite plutons intruded into higher density gneissic rocks.

The location and geologic setting of Payette National Forest in west-central Idaho is shown on figure 1. For reference, small scale Bouguer gravity anomaly and total-intensity aeromagnetic anomaly maps of the region (figs. 2 & 3) are presented to show the basic aeromagnetic and gravity anomaly fields that are later enhanced and interpreted in the report.

### Previous Studies

Aeromagnetic and gravity anomaly maps have been published previously in conjunction with mineral resource and geologic framework investigations of the northern Rocky Mountains and provide a regional aeromagnetic and gravity background for study of PNF (Bankey, 1992; Bankey and others, 1985; Bankey and Kleinkopf, 1988; Cady and others, 1990; Eaton and others, 1978; Kleinkopf, 1998; Mabey, 1982; Mabey and Webring, 1985; Mabey and Tschanz, 1986; Mabey and others, 1978; McCafferty, 1992; Zietz and others, 1971 and 1978). Interpretations by A. Griscom and D. Kleinkopf were made of aeromagnetic and gravity anomaly data of the Elk City 1° x 2° quadrangle that extends from lat 45°N. - 46°N. and long 114°W. - 116°W., as part of a USGS preliminary mineral resource assessment (Lund and others, 1990). The Payette National Forest extends into the southwestern part of the Elk City quadrangle.

## GEOPHYSICS

### Physical Properties of Rocks

Estimates of density and magnetic susceptibility values judged to be representative of the major lithologic units are based on three sources: (1) new laboratory and field measurements; (2) values obtained by Mabey and Webring (1985) from their studies of the Challis CUSMAP quadrangle, and (3) values obtained by Criss and Champion (1984) from analyses of more than 600 samples of granitic rocks collected in the southern part of the

Idaho batholith to study effects of hydrothermal alteration on the magnetic properties. Rock densities and magnetic susceptibilities used for the interpretations are given in table 1.

Densities of Cretaceous granodiorite and two-mica granite that make up the main part of the Idaho batholith (Lund and others, 1997) average 2.60 g/cm$^3$. Tonalite and diorite intrusions are about 2.68 g/cm$^3$. Densities of Cenozoic sedimentary and Tertiary volcanic rocks are less than 2.6 g/cm$^3$; however, the volcanic rocks show large variations in density and magnetization. The Tertiary granites average about 2.57 g/cm$^3$, which is slightly less than the Cretaceous granites. Paleozoic sedimentary rocks in the eastern part of the study area that occur as roof pendants in late Cretaceous plutons of the Idaho batholith (Lund and others, 1997) average about 2.56 g/cm$^3$ ; Precambrian metasedimentary rocks average 2.71 g/cm$^3$ (table 1). The low density of granitic rocks of the Tertiary batholiths and stocks appears to be related to extensive hydrothermal alteration. Criss and Champion (1984) concluded that pervasive hydrothermal alteration is often associated with the Tertiary granitic intrusions and appears to cause minor lowering, on the order of 0.02-0.04 g/cm$^3$, of the bulk density of most lithologies.

Granitic rocks of the Tertiary (Eocene) epizonal plutons, located in the eastern part of the forest, were observed by Mabey and Webring (1985) to have a higher magnetic susceptibility (180 x $10^{-5}$ cgs units) than granodiorite rocks of the Cretaceous Idaho batholith interior (50 x $10^{-5}$ cgs units). Criss and Champion (1984) measured the magnetic susceptibility of Cretaceous granodiorite and two-mica granite rocks from the same general interior area of the batholith and found them weakly magnetic, with values ranging from 1 to 46 x $10^{-5}$ cgs units. They observed few measurable magnetic high anomalies associated with Cretaceous plutonic rocks of the batholith interior (Criss and Champion, 1984; also see figure 7, this report). Distinct aeromagnetic highs are associated with diorite and tonolite rocks that occur along the western border phases of the Idaho batholith and Salmon River Suture (figs. 3, 4, 6, & 7) . Griscom (Written commun., 1990) studied the western border phases of the Idaho batholith and confirmed from plots of low-level NURE magnetic flight profiles that a boundary can be drawn between magnetite bearing rocks along the western of the Idaho batholith and the ilmenite bearing rocks of the central portion, as postulated from petrologic studies by Piccoli and Hyndman (1985) and discussed by Criss and Champion (1984). The magnetite-ilmenite boundary is along the eastern margin of the Salmon River Suture zone that is nearly coincident with the initial strontium isotope ratio ($Sr^{87}/Sr^{86}$) line that indicates oceanic values of $<.704$ west of line and continental values of $>.706$ east of line (Lund and others, 1997).

The late Tertiary Columbia River Basalts are in most places moderately to strongly magnetic. Prieto and others (1985) in their model studies used an average value for magnetic susceptibility of 300 x $10^{-5}$ cgs units, compared to an average value of 670 x $10^{-5}$ cgs units determined in this study. These extrusive volcanic rocks may be observed locally to exhibit greater remanent magnetization than induced magnetization by several orders of magnitude. However, for most Cretaceous and Tertiary plutonic rocks of the batholith, Criss and Champion (1984) found low Koenigsberger ratio values in laboratory measurements. They concluded that remanent magnetizations are negligible relative to magnetic susceptibility in interpretations of most aeromagnetic anomalies of the region.

Proterozoic to Paleozoic rocks located in the eastern part of the Payette National Forest study area (Lund and others, 1990) are roof pendants composed mainly of meta-sedimentary rocks. These rocks are nonmagnetic (Maby and Webring, 1985), except for local enrichment of magnetite in hydrothermally altered areas around Tertiary intrusions (Criss and Champion, 1984)

**Table 1 -- Density and magnetic susceptibilities of major rock types**

| Rock types | Density g/cm$^3$ | Density Range (samples) | Magnetic susceptibility $10^5$ cgs units | Range (samples) |
|---|---|---|---|---|
| Tertiary Columbia River basalt[3] | 2.86 | 2.84 - 2.89 (4) | 670 | 70 - 1893 (4) |
| Tertiary Columbia River basalt[4] | 3.00 | | 300 | 23 - 770 |
| Tertiary granites[1] | 2.57 | 2.55 - 2.61 (14) | 63 | 23 - 139 (14) |
| Tertiary Panther Creek volcanics[2] | 2.33 | | 110 | |
| Tertiary Challis volcanics[2] | 2.46 | | 220 | |
| Tertiary rhyolites[3] | 2.59 | 2.58 - 2.61 (4) | 12 | 2 - 29 (4) |
| Teritary Castro pluton[2] | 2.58 | | 180 | |
| Cretaceous tonalites & diorites - west side IB[1] | 2.68 | 2.62 - 2.73 (20) | 40 | 1 - 145 (20) |
| Cretaceous granites - interior IB[1] | 2.60 | 2.56 - 263 (38) | 10 | 1 - 46 (38) |
| Cretaceous IB granodiorite[2] | 2.58 | | 50 | |
| Cretaceous IB tonalite[2] | 2.67 | | 100 | |
| Paleozoic sedimentary rocks[2] | 2.56 | | ------- | |
| Precambrian metasedimentary rocks[3] | 2.71 | 2.69 - 2.71 (4) | 26 | 14 - 48 (4) |

1 - Criss and Champion, 1984; 2 - Mabey and Webring, 1985; 3 - Current study; 4 - Prieto and others, 1985

## Aeromagnetic Data

Total-intensity aeromagnetic data covering the Payette National Forest were extracted from gridded data compiled by McCafferty (1992) for use in mineral resource assessment project studies of the Idaho batholith and adjacent areas. Procedures for mathematically reducing and merging data from individual surveys to a common level of about 300 m (1,000 ft) above ground are described by McCafferty ( 1992). The study area is covered by parts of six individual aeromagnetic surveys. Flight altitude ranged from 120 m (400 ft) above terrain to 3,350 m (11,000 ft) barometric and with line spacings ranging from 0.8 to 3.2 km (0.5 to 2.0 mi.). The complete data set (McCafferty, 1992) is available in digital format from the National Geophysical Data Center (NGDC), National Oceanic and Atmospheric Administration (NOAA), Boulder, CO 80303.

Other aeromagnetic data that cover the Payette National Forest are from reconnaissance surveys of the Baker, Elk City, Challis, and Grangeville 1° x 2° quadrangles, made as part of the National Uranium Resource Evaluation (NURE) program of the U.S. Department of Energy. The NURE aeromagnetic anomaly maps are available from the U.S. Geological Survey in NURE reports GJBX-010(80), GJBX-101(78), GJBX-156(79), and GJBX-098(81) (EG&G geoMetrics, 1979; Geodata International, Inc., 1978, 1979, & 1981; Hill, 1986).

The total-intensity aeromagnetic anomaly data (fig. 3) were reduced to the pole. Residual anomaly maps (figs. 4 and 7) and pseudo gravity gradient data were prepared to enhance anomalies for purposes of the geologic interpretation. The processing was done with software that uses fast fourier transforms to convert aeromagnetic anomaly data in the space domain to the frequency domain (Hildenbrand, 1983). The reduced to the pole data corrects anomaly locations for inclination of the earth's magnetic field (about 69°) and shifts anomaly centers over the causative sources.

The residual aeromagnetic anomaly maps, in shaded relief, (figs. 4 and 7) were prepared by wave-length filtering (50 km high pass) the total-intensity data that had been reduced-to-the-pole. The filtering emphasizes anomalies due to sources in the upper crust, on the assumption that anomaly wavelength is proportional to depth of source (Bankey and Kleinkopf, 1988; Hildenbrand, 1983). The traces of gradient midpoint of the horizontal gradient of the pseudo gravity (figs. 4 and 7) were calculated and plotted on the residual aeromagnetic anomaly maps to help delineate magnetization boundaries (Cordell and Grauch, 1985) that may signify geologic contacts or linear geologic features, such as faults or dikes. The pseudogravity is computed from the total-intensity aeromagnetics (Hildenbrand, 1983; Baranov, 1957).

### Gravity Data

The Bouguer gravity anomaly data covering the region that includes the Payette National Forest (fig. 2) were extracted from an earlier compilation prepared for regional mineral resource assessment of the Idaho batholith and adjacent areas (Bankey, 1992). Additional control consisting of 28 gravity observations was provided by D. Kulik (Written commun., 1994) and 178 new gravity readings were made by the author during the 1992 and 1993 field seasons. The total gravity control for the Bouguer gravity anomaly map region (fig. 2) consists of about 6,450 unevenly spaced stations mainly along roads and trails.

The observed gravity values are referenced to the IGSN-71 gravity datum (Morelli and others, 1974) and are based on the 1967 ellipsoid (International Association of Geodesy, 1971). The details of reducing the Bouguer gravity anomaly data (fig. 2) and preparing the isostatic residual gravity anomaly data are described by Bankey (1992). All gravity stations were corrected for terrain effects out to a radius of 167 km using the method of Plouff (1977). The digital gravity data may be obtained from the National Geophysical Data Center (NGDC), National Oceanic and Atmospheric Administration (NOAA), Boulder, CO 80303.

A high pass isostatic residual gravity anomaly map, in shaded relief, (fig. 8) was prepared using a high pass wave-length filter with a cut off of 50 km (Hildenbrand, 1983) in order to enhance and separate subtle gravity anomalies that may help isolate igneous intrusions or other discrete rock masses.

## GEOLOGY

In the middle Proterozoic, sedimentary rocks of the Belt Supergroup in western Montana and northern Idaho were deposited in the Belt basin which formed part of an epicratonic reentrant along the eastern edge of the Cordilleran miogeocline (Harrison, 1972). Belt rocks consist of Middle Proterozic metasedimentary rocks that are preserved as roof pendants on the Idaho batholith in the eastern part of the Payette National Forest (See map unit Y, fig. 6; Lund and others, 1997).

Figure 3 shows the approximate location of the three geologic terranes that span the Payette National Forest. The terranes, from east to west, are 1) the Idaho batholith granitic terrane along the western edge of the North American continental craton, 2) terrane of the Salmon River suture zone of deformation (Lund, 1988) and, 3) the allochthonous island-arc terrane of oceanic origin, consisting of metamorphosed plutonic and volcanogenic clastic and carbonate rocks of the Blue Mountain volcanic arc (Vallier and Brooks, 1986), that were accreted to the craton (Lund and others, 1997) along the Salmon River suture. Basalt flows of the Miocene Columbia River Basalt Group (Trc, fig. 6) occur in extensive areas of the accreted terrane and in local areas along the Salmon River Suture zone (figs 3 & 6).

The geology (fig.6) referred to in the discussions of the aeromagnetic and gravity anomalies (figs. 7 & 8) is modified from Karen Lund (Written commun., 1998), which she generalized from her 1:100,000 scale geologic compilation prepared for the Payette National Fores (Lund and others, 1998).

## INTERPRETATION OF REGIONAL AEROMAGNETIC ANOMALY DATA

The aeromagnetic patterns on the residual anomaly map (fig. 4) of the region reflect the diverse lithologies and structures of the southern part of the Idaho batholith and adjacent accreted terranes. The terranes discussed in the geology section are shown on figures 3 and 4. Trends on the map are plotted from traces of midpoints of anomaly gradients described in the section on aeromagnetic data. They help delineate magnetization boundaries (Cordell and Grauch, 1985) that may indicate geologic contacts around intrusions or traces of linear geologic features, such as faults or dikes. High-amplitude, high-intensity anomaly fields, and high gradient trends characterize the volcanic rocks of the accreted terrane on the west and the Snake River Plain on the south. The dominantly Cretaceous muscovite-biotite granite and hornblende biotite granodiorite of the interior part of the batholith exhibit low gradient anomalies. Along the western border, prominent, north-south elongated magnetic highs reflect tonalitic and dioritic rocks that are part of and marginal to the pre-batholith Salmon River suture (fig.4). Eocene granitic rocks occur throughout the Idaho batholith, but are of high magnetic susceptibility (table 1) and are readily distinguished from the less magnetic Cretaceous granitic rocks.

Mineralized areas of the Idaho batholith often correlate with fault systems, shear zones, and volcanic calderas that are expressed in the aeromagnetic anomaly data. Of particular importance are two regional mineralized trends, the trans-Challis fault system (TCFS) described by Kiilsgaard and Bennett (1985) and the central Idaho mineral belt (CIMB), proposed by D.H. Adair (1988). These mineral belts are expressed as discontinuous and parallel high gradient zones, and discrete and complex magnetic highs and lows in the and may have impacted the mineral endowment of the eastern part of the Payette National Forest (fig. 4) where they intersect. The trans-Challis fault system (TCFS) is described by Kiilsgaard and Bennett (1985) as a major zone of Eocene rifting and crustal extension that extends from near lat 45° 30' N and long 114° W. southwest across the Idaho batholith terrane for more than 300 km, and possibly beneath lavas of the Snake River Plain to lat 43° N and long 117° W. The aeromagnetic expressions along the trans-Challis fault system are associated with igneous intrusions and calderas, such as structures of the Boise basin, Custer graben, Castro pluton, Twin Peaks caldera, and the Panther Creek graben (fig. 4). The zone may continue northeast of the Panther Creek graben as part of the Great Falls lineament that extends northeast across Montana, as proposed by O'Neill and Lopez (1985). Interpretations of anomalies along the trans-Challis fault system, made in connection with USGS mineral assessments of public lands, indicate that the igneous intrusions and calderas may broaden and provide extensive host rock for mineral deposits in the subsurface (Kiilsgaard and others, 1985; Mabey and Webring, 1985; Fisher and others, 1992).

The north-northwest trending central Idaho mineral belt (CIMB) is based on alignments of clusters of lode mines and prospects in central Idaho (D.H. Adair, Written commun., 1988). The central Idaho mineral belt intersects the trans-Challis fault system at the Thunder Mountain Caldera and the Stibnite mining district. Patterns of the traces of aeromagnetic gradient midpoints help define faults and igneous intrusions along the central Idaho mineral belt that extends across the Payette National Forest to include the Warren and Elk City mining districts (fig. 4). The correlative evidence in the aeromagnetic data may warrant further studies data along these mineral belts.

## INTERPRETATION OF AEROMAGNETIC ANOMALY DATA FOR PAYETTE NATIONAL FOREST

The residual aeromagnetic anomaly map with superimposed trends from traces of gradient midpoints (fig. 7) exhibits signatures of specific geologic units and forms the basis for discussion in this report. Anomalies discussed in the text are identified by numbers M1-M20 on figure 7. The residual aeromagnetic anomaly map of the forest (fig. 7) is an enlargement of the smaller scale regional aeromagnetic map (fig. 4) and at the same scale can be readily compared with the geologic map (fig. 6). The plots of traces of the midpoints of the pseudo gravity gradients help define magnetization boundaries (Cordell and Grauch, 1985) that may be interpreted as geologic contacts around intrusions or fault zones (fig. 7).

Broad areas of Cretaceous Idaho batholith granitic terrane (Kg) exhibit a low relief magnetic field east of long 116° W. (M1). Low amplitude anomalies (about 50 nT) of various orientations in the area reflect inferred granodiorite phases (M2) of the Kg unit (fig 6 &Lund and others, 1997) that are more magnetic than the extensive muscovite and biotite granite phases characterized by high ilmenite/magnetite ratios (Piccoli and Hyndman, 1985). In the east-central part of the study area, three aeromagnetic highs (M3, M 4, & M5) correlate with outcrops of syenite and diorite (OZ) of Ordovician to Upper Proterozoic age (fig. 6 & Lund and others, 1990). The central magnetic high (M3) has an amplitude of about 800 nT. The anomaly source (OZ) appears to be extensive and probably is continuous in the subsurface based on northwest aligned outcrops of syenite and diorite (OZ) and corresponding magnetic highs (M4 & M5). In the northeast part of the PNF, in an area of Tertiary granite (Tg), the aeromagnetic anomaly data exhibit low gradients, except for a distinctive high (M6) of about 100 nT that trends northeasterly. The high is inferred to reflect a phase of Tertiary intrusive rock that is more magnetic than adjacent granitic rocks mapped as Tertiary age (fig. 6). The alternative is that the adjacent relatively non-magnetic granites are of Cretaceous age and are of low magnetic susceptibility, in accordance with the findings of Mabey and Webring (1985) that are discussed in the section on physical properties (table 1).

Challis volcanics (Tc), overlie and bury the Thunder Mountain Caldera (Leonard and Marvin, 1984). An approximate outline of the Thunder Mountain Caldera is shown on figure 4. The volcanics exhibit a relatively low-gradient field (northeast and northwest of anomaly M7) that is punctuated by several small magnetic highs (fig. 7) inferred to reflect igneous intrusions in the cauldron complex (figs. 4 & 6). The alignment of aeromagnetic highs in the central part of the caldera suggests that postulated igneous intrusions may occur along a structural zone described earlier as part of the trans-Challis fault system (fig. 4). The zone may project from the Profile Gap-Smith Creek dike swarm shown on figure 6 at a location of about 5 km southwest of the forest boundary. For more detail see Lund and others (1997). The dike swarm intersects the south margin of the volcanic terrane (M7). Along the eastern margin of the Thunder Mountain Caldera (figs. 3, 4 & 6), the Castro Pluton (Tg) displays an irregular anomaly pattern of aeromagnetic highs and lows (M8) and is probably related to different stages of hydrothermal alteration along the caldera-pluton contact (Leonard and Marvin, 1984). Other small outcrops of granite (Kg and Tg) along the southwest and west margin (M9) of the Thunder Mountain Caldera exhibit small aeromagnetic highs in some cases and in other cases no evident expression. An outcrop of Tertiary granite (Tg) along the west side of the caldera exhibits a distinctive aeromagnetic high of 50-100 nT (M10) that is smaller, but similar in cross-trend to the anomaly of the postulated Tertiary granitic intrusion labeled M6.

In the central part of the study area along the western margin of the Idaho batholith, north-trending aeromagnetic patterns and short wave-length anomalies (M11) reflect rocks of intermediate to mafic composition (Kgdf, Kgn) associated with the Salmon River Suture (fig. 6 & Lund and others, 1997). A well defined linear aeromagnetic high (M12) correlates with north-south trending faults and tonalite rocks of the suture zone (figs. 4 & 6). Traces of the midpoints of the high gradient zones help define the extent of the faults. The complex of aeromagnetic highs and lows along the suture zone (figs. 4 & 7) mainly reflects variations in magnetization of tonalite and granodiorite (fig. 6, see Kgdf, Kgn) and reflects the complexity of geologic structure and different lithologies along the suture.

In the allochthonous island arc-volcanic terrane, located in the western part of the study area, many of the aeromagnetic highs correlate with outcrops of Columbia River basalt (Tcr, fig. 6). Anomaly trends often parallel fault zones (figs. 6 & 7). In the central part (M13), north-trending faults (fig. 6) are reflected in the aeromagnetic anomaly and high magnetic gradient zone patterns. In the southwest part of the Payette National Forest (figs.4 and

7) and adjacent areas in the broad valley to the southeast (fig. 5) nearly equidimensional magnetic highs (M14, M15) correlate with outcrops of Columbia River basalt (Tcr) and Basalt of Weiser (Tw). Sources of two prominent aeromagnetic highs located east of M14 and south of M15 are inferred to be shallow basalt beneath sedimentary rocks of the Payette Formation (Tp).

A distinctive aeromagnetic high (M16) that trends north to north-northwest occurs over Columbia River basalt and Quaternary sediments (Q) in the northeast part of a small valley of Quaternary sediments (figs. 7). The high intensity anomalies suggest that the sediments are thin and underlain by highly magnetic basalt in this area (figs. 6 & 7). The traces of high gradient zones re-enforce linear trends on the residual anomaly map (fig. 7) and suggest the presence of a buried valley or graben of thickened basalt that continues north-northwest and is cut-off by northeast trending faults (M17).

To the north a complex aeromagnetic high (M18) trends north-northeast about 15 km and correlates with outcrops, and inferred subcrops, of granodiorite, diorites, and gabbro rocks (fig. 6, Kjqd). Mafic rocks of the Wallowa terrane (W) may contribute to some component of the high magnetic intensities. This complex magnetic ridge extends north-northeast intermittently over a distance of some 50 km and the magnetic rock distribution may be controlled by north-northeast trending fault zones, as suggested by the high magnetic gradient zone plots. To the northwest, complex highs (M19) trend north to northwest, but do not cross the Snake River. These two aeromagnetic highs (M19) that correlate in part with northwest trending outcrops of Kjqd, suggest that mafic lithologies of Kjqd are more extensive in the subsurface. West of the river (M20), aeromagnetic patterns parallel the river and are similiar to complex patterns east of the river where northwest oriented highs (M19) correlate with metavolcanic rocks of Wallowa terrane (W) and Cretaceous mafic intrusions (fig. 6 - Kjqd).

## AEROMAGNETIC ANOMALIES AND PERMISSIVE TRACTS FOR MINERAL DEPOSIT MODELS

The USGS Payette Forest minerals assessment team, using a consensus of interpretations of geologic, geophysical, geochemical, radioelement, and remote sensing data, prepared permissive tract maps of mineral resource deposit models that might be expected to occur in Payette National Forest. The outlines of permissive tracts for four of the mineral deposit models (DM1-DM4) used by the USGS team in the assessment are plotted on the residual aeromagnetic anomaly map (fig. 7). The description of the mineral deposits that occur and the procedures used in the mineral assessment are discussed in detail by Bookstrom and others (1998). Interpretations of the aeromagnetic anomaly data, and to some extent the gravity anomaly data, provided constraints on the subsurface distribution of bedrock geology and fault zones that may relate to the occurrence and distribution of mineral resources. Permissive tracts were delineated normally in areas of mineral occurrences that exhibited significant aeromagnetic and geochemical anomalies and geological conditions favorable for the occurrence of mineral desposits. The aeromagnetic patterns for each of the four deposit models are discussed below:

1) Copper, molybdenum, tourmaline greissen breccia pipes. The aeromagnetic signature for these porphyry copper-molybdenum resources is characterized by three deep aeromagnetic lows that are interpreted to

reflect chaotic and altered rocks of breccia pipes. Other aeromagnetic lows in the western part of the map may be worthy of investigation, but did not define tract boundaries due to lack of evidence from the other disciplines.

2) Podoform chromite and diamond pipes. Linear and equidimensional aeromagnetic anomalies and high aeromagnetic gradients zones along the Salmon River Suture suggest elongate and circular geologic features and the presence of mafic rocks that may warrant further investigation (figs. 6 and 7). The prominent lows in the southern part should be investigated for evidence of indicator minerals that may signal the presence of kimberlite pipes, thus providing possibilities for the occurrence of diamonds. High amplitude linear positive anomalies (M12) in the northern part of the tract may reflect mafic rocks favorable for hosting podoform chromite.

3) Permissive host rocks for Au, Ag, and Cu. The distribution of small anomalies of various trends suggests possibly a large buried igneous complex , possibly of Tertiary age that probably is not related to older dioritic and syenitic intrusions expressed by the high intensity anomalies (M3, M4, and M5) on the northeast side of the tract.

4) Polymetallic veins. This relatively low magnetic gradient area is punctuated by small prominent dipole magnetic anomalies that suggest shallow Tertiary pluton sources that might host mineralization in the area.

## INTERPRETATIONS OF GRAVITY ANOMALY DATA FOR THE PAYETTE NATIONAL FOREST

The Bouguer gravity anomaly map (fig. 2) of the region of the Payette National Forest provides an overview of the gravity field for the southern part of the Idaho batholith. The low values show a strong inverse correlation with high topography (Mabey and Webring, 1985). The regional low (fig. 2) reflects an approximate isostatic balance of the batholith, and according to Mabey and Webring (1985) much of the negative mass anomaly probably results from a thickened crust beneath central Idaho. The Bouguer gravity anomaly map (fig. 2) shows that the gravity field is some 50 mGal higher in the western part of the forest over high density oceanic and volcanic rocks compared to the low-density granitic terrain in the eastern part of the forest. For the interpretations, an isostatic anomaly map described in the section on gravity data was prepared in order to resolve subtle anomalies from local sources in the upper part of the crust. The gravity anomaly data, in some cases, provided constraints on the interpretations of the aeromagnetic anomaly data in applications to the mineral resource assessment.

The high pass isostatic residual gravity anomaly map (fig. 8) enhances subtle anomalies that may relate to different rock types at the surface and in the subsurface. In particular, low amplitude anomalies are observed to result from subtle density differences between most of the Cretaceous and Tertiary granites, 2.6 g/cm$^3$ versus 2.57 g/cm$^3$ (table 1; Criss and Champion, 1984). Density contrasts may be due to different mineral phases within major granitic units, such as Tg and Kg (fig. 6 & Lund and others, 1997).

Prominent isostatic gravity highs and lows on the map (fig. 8) are attributed to several different sources. In the Idaho batholith terrane, distinct gravity lows (G1) correlate generally with mapped biotite-muscovite granite of the Kg unit (figs. 6 & 8; for details, see Lund and others, 1997). The low field intensity of the four anomalies labeled G1 probably reflect the thickest part of the biotite-muscovite granite (mainly Kg). At G2, higher gravity values based on limited control correlate with a low amplitude aeromagnetic high (fig. 7). The source of the weak gravity high and corresponding aeromagnetic high is interpreted to be a more granodioritic phase in the Kg unit. Two gravity lows (G3) correlate with the central part of the Challis Volcanic field (fig. 6) at the Thunder Mountain Caldera (Leonard and Marvin, 1984). The lows are interpreted to reflect the low density volcanic debris (table 1) in the caldera. The gravity low (G4) in the northeastern part of Payette National Forest generally correlates with the aeromagnetic ridge (anomaly 6 on figure 7) that reflects magnetic rocks within the broad area of Tertiary granite (Tg, fig. 6), or possibly unmapped Cretaceous granitic rocks. The correlation of an aeromagnetic high with a gravity low is interpreted to reflect Tertiary granitic plutons in Cretaceous Idaho batholith granite, since Tertiary granites were found to have higher magnetic susceptibility than Cretaceous granites and lower density (table 1). High anomalies G5 and G6 are not explained by the surface geology that consists of relatively non-magnetic Cretaceous granitic rocks. The Tertiary granite is less dense than the Cretaceous granites (table 1) and is therefore not considered a source for the 5 to 7 mGal amplitude positive anomalies (fig. 8). Because the aeromagnetic anomaly data show no distinct correlative anomalies, the sources of gravity highs G5 and G6 are unknown, but may be high density felsic Precambrian crystalline rocks of Pre-Cretaceous Idaho batholith metamorphic basement complex. Gravity highs G7, G8, and G9 show some correlation with aeromagnetic highs (fig. 7), which suggests that the sources may be high density mafic phases of the Cretaceous granites.

The isostatic anomalies (G10) within the suture zone correlate in trend with the north-trending aeromagnetic highs described earlier (fig. 7, M12), except the gravity anomalies generally are of longer wave-length which may be partly a function of wide spaced control in this area. Anomaly areas G10 correlate mainly with tonalite rocks (fig. 6, Kgdf) of the Salmon River Suture. The northern anomaly (G10) does cover an outcrop of Columbia River Basalt (fig. 6, Tcr), which may account for part of the anomaly. The deep low in the southern part of the suture zone (G11, fig. 8) is inferred to reflect low density alluvial deposits of Long Valley (Schmidt and Mackin, 1970). This gravity low of more than 15 mGal amplitude suggests a thickness of at least 500 m. of unconsolidated sediments for the source of the anomaly. A density contrast is assumed of about 0.5 g/cm$^3$ between alluvial deposits (fig. 6, Q) and granitic rocks (fig. 6, Kgdf and Kgn). The northeast trending low (G12) approximately parallels a thrust fault (fig. 6) along the northeastern edge of the forest and correlates with mapped metavolcanic and volcanogenic rocks (TrJ, fig. 6). A northeast-trending aeromagnetic low (fig. 7) generally correlates with the gravity low at G12.

The isostatic gravity anomaly patterns of the island arc volcanic terrane (figs. 6 & 8) are generally similar to the patterns of the aeromagnetic map (figs. 7). Gravity highs G13-G17 are inferred to reflect high density basalts (Tcr) with which they correlate (figs. 6 and 8). A north-south trending low (G18) that is over a topographic low (fig. 5) is inferred to reflect a faulted geologic complex of metavolcanic and volcanogenic rocks (fig. 6). The source for the isostatic gravity lows (G19, G20) along the west side of the Payette National Forest are interpreted to be relatively low density and variable magnetic susceptibility rocks of Island Arc Wallowa (W), Olds Ferry (O), and Izee (I) terranes (figs. 7 & 8) are preserved in a possible structural depression covered by a veneer of Columbia River Basalt (Tcr) . The scattered outcrops of island arc rocks are probably severely tectonically deformed in the subsurface resulting in lowering of their density and magnetic susceptibilities (figs. 6, 7, and 8). A gravity low (G21) located in the southwest part of the study area is inferred to reflect low density Payette Formation sedimentary rocks (fig. 6 and 8) that may be wide spread beneath Weiser basalt (Tw) in a broad valley (fig 5). Thus, the enhanced anomalies of the high pass isostatic residual map (fig. 8) provides additional detail within the broad anomaly areas of the Bouguer gravity anomaly map (fig. 2).

## CONCLUSIONS

1) The aeromagnetic and gravity anomaly maps were used in the team assessment process to help outline permissive tracts for the mineral deposits models based on combined interpretations of geological, geochemical, radioelement, and thematic mapper data.

2) The aeromagnetic anomaly maps provided more specific information than the gravity anomaly maps about buried structure and igneous intrusive rocks that might influence localization of undiscovered mineral deposits, largely due to the greater density of control collected along aeromagnetic profiles compared to the 3-4 km randomly spaced gravity observation points.

3) The aeromagnetic anomaly maps were used help set the limits of tract outlines in areas beyond localities of mineral occurrences, or geochemical anomalies.

4) The gravity anomaly maps in the mineral assessment process provided constraints and supplemental information for the aeromagnetic interpretations, such as fault controlled distribution of volcanic rocks in the accreted terrane.

5) The boundaries of the three north-south trending geologic terranes that span the forest were refined by distinctive aeromagnetic signatures characteristic of each terrane: a) the Idaho batholith granitic terrane, b) the Salmon River suture zone terrane, and c) the allochthonous island-arc and Columbia River basalt terrane.

6) Two regional mineralized trends are of particular importance. The trans-Challis fault system (TCFS) and the central Idaho mineral belt (CIMB) are regional geologic features composed of zones of mineral localities, igneous intrusions, and faults zones that have expressions in the aeromagnetic anomaly data as discontinuous aligned gradient zones and linear distributions of anomalies. These regional mineral belts may have impacted the mineral endowment of the eastern part of the Payette National Forest, where they intersect. The aeromagnetic data are worthy of further study to identify other possible buried structure and igneous intrusions along these mineralized trends.

7) The data and concepts presented in this report form the basis for investigations of the distribution and genesis of the mineral deposits of the southern part of the Cretacous Idaho batholith and for research into the emplacement of the batholith along the Salmon River suture zone that formed when pre-batholithic oceanic terrane was accreted to the western edge of the continental craton.

## ACKNOWLEDGMENTS

I thank Bob Bryan (retired), former Minerals Program Manager for the Payette National Forest, for his cooperation and logistical support, which was particularly helpful during periods that we conducted field work in 1992 and 1993. Members of the minerals team provided data and discussion that were valuable background for this report, namely, Art Bookstrom, Terry Cookro, Bruce Johnson, Harley King, Karen Lund, Sussane Miller, Jim Pitkin, David Sanchez, and Ken Watts. Ron Worl advised about interfacing with Payette National Forest management at the beginning of the geophysical work. Jane Stone and Deb Parliman of the USGS Water Resources Division Boise office, gave insights about the southern part of Long Valley from seismic modeling and geochemical modeling. Earl Bennett, Director of the Idaho Geological Survey, provided perspective about the geological and geophysical problems of the Idaho batholith.

## REFERENCES

Adair, D.H., 1988, The evolution of mineral belts in central Idaho: Program, Northwest Mining Association 94th Annual Meeting, December 3, 1988, Spokane, Washington.

Bankey, Viki, 1992, Complete Bouguer gravity, isostatic residual gravity, and related geophysical maps centered on the Idaho batholith and Challis volcanic field, northwestern United States: U.S. Geological Survey Geophysical Investigations Map GP-995, 2 sheets.

Bankey, Viki and Kleinkopf, M. Dean, 1988, Bouguer gravity anomaly map and four derivatives of Idaho: U.S. Geological Survey Geophysical Investigations Map GP-978.

Bankey, Viki, Webring, M.W., Mabey, D.R., Kleinkopf, M.D., and Bennett, E.H., 1985, Complete Bouguer anomaly map of Idaho: U.S. Geological Survey Miscellaneous Field Investigations map MF-1773.

Baranov, V., 1957, A new method for interpretation of aeromagnetic maps: pseudo-gravimetric anomalies: Geophysics, v. 22, p. 359-383.

Bookstrom, Arthur A., Johnson, Bruce R., Cookro, Theresa M., Lund, Karen, Watts, Kenneth, C., King, Harley D., Kleinkopf, Merlin D., Pitkin, James A. Sanchez, David J., and Causey, J. Douglas, in prep. 1998, Mineral resource assessment of the Payette National Forest, West-Central Idaho: U.S. Geological Survey Open-File Report 98-xx.

Cady, J.W., Bankey, Viki, Lee, Keenan, McCafferty, A.E., Pitkin, J.A., and Stanley, W.R., 1990, Synthesis of geophysical and geological data centered on the Idaho batholith and the Challis volcanic field, Idaho: [abs.], *in* Good, E.E., Slack, J.F., and Kotra, R.K., eds., USGS research on mineral resources--1991, Program and abstracts, 7th Annual V.E. McKelvey Forum on mineral and energy resources: U.S. Geological Survey Circular 1062, p. 6-7.

Cordell, L.E. and Grauch, V.J.S., 1985, Mapping basement and magnetization zones in the San Juan basin, New Mexico, in, Hinze, W.J., ed., The utility of regional gravity and magnetic maps: Tulsa, Society of Exploration Geophysicists, p. 181-197.

Criss, R.E., and Champion, D.E., 1984, Magnetic properties of granitic rocks from the southern half of the Idaho batholith--Influences of hydrothermal alteration and implications from aeromagnetic interpretation: Journal of Geophysical Research, v. 89, no. B8, p. 7061-7076.

Eaton, G.P., Wahl, R.R., Proska, H.J., Mabey, D.R., and Kleinkopf, M.D., 1978, Regional gravity and tectonic patterns - their relation to Late Cenozoic epeirogeny and lateral spreading in the western Cordillera, *in* Smith, R.B., and Eaton, G.P., eds., Cenozoic tectonic and regional geophysics of the western Cordillera: Geological Society of America Memoir 152, p. 251-291.

EG&G geoMetrics, 1979, Aerial gamma ray and magnetic survey, Idaho project, Hailey, Idaho Falls, and Elk City quadrangles of Idaho/Montana, and Boise quadrangle, Oregon/Idaho: U.S. Department of Energy, Grand Junction Office Report GJBX-010(80), 4 vols., variously paginated.

Geodata International, Inc., 1978, Aerial radiometric and magnetic survey, Baker national topographic map, Idaho and Oregon: U.S. Department of Energy, Grand Junction Office Report GJBX-101(78), 2 vols, variously paginated.

______________________________, 1979, Aerial radiometric and magnetic survey, Challis national topographic map, Idaho: U.S. Department of Energy, Grand Junction Office Report GJBX-156(79), 2 vols, variously paginated.

______________________________, 1981, Aerial radiometric and magnetic survey, Grangeville Topographic Map, Idaho-Oregon-Washington: U.S. Department of Energy, Grand Junction Office Report GJBX-098(81), 1 vol, variously paginated.

Fisher, F.S., McIntyre, D.H., and Johnson, K.M., 1992, Geologic map of the Challis 1° x 2° quadrangle, Idaho: Miscellaneous Investigation Series Map I-1819, scale 1:250,000, pamphlet 39 p.

Harrison, J.E., 1972, Precambrian Belt basin of northwestern United States -- Its geometry, sedimentation, and copper occurrences: Geological Society of America Bulletin, v. 83, no. 5, p. 1215-1240.

Hildenbrand, T. G., 1983, FFTFIL: A filtering program based on two-dimensional Fourier analysis of geophysical data: U.S. Geological Survey Open-File report, 83-237.

Hill, P.L., 1986, Lists and location maps of aeromagnetic and aeroradiometric publications from the Department of Energy NURE program: U.S. Geological Survey Open-File Report 86-525-G, 22 p.

International Association of Geodesy, 1971, The Geodetic Reference System, 1967: International Association of Geodesy Special Publication no. 3, 116 p.

Kiilsgaard, Thor H. and Bennett, Earl H., 1985, Mineral deposits in the southern part of the Atlanta Lobe of the Idaho batholith and their genetic relation to Tertiary intrusive rocks and to faults, *in* D.H. McIntyre, ed., Symposium on the geology and mineral deposits of the Challis quadrangle, Idaho: U.S. Geological Survey Bulletin 1658-E, p. 153-165.

King, P.B., 1962, Tectonic map of United States: U.S. Geological Survey and American Association of Petroleum Geologists, scale 1:2,500,000, 2 sheets.

Kleinkopf, M. Dean, 1998, Interpretation of regional aeromagnetic and gravity anomalies, Belt-Purcell terrane and adjacent areas, northern Rocky Mountains, United States and Canada, *in* Berg, Richard B., ed., Proceedings of Belt II Symposium: Montana Bureau of Mines and Geology, Special Publication 112.

Leonard, B.F. and Marvin, R.F., 1984, Temporal evolution of the Thunder Mountain caldera and related features, central Idaho, *in* Bill Bonnichsen and R.M. Breckenridge, editors, Cenozoic Geology of Idaho: Idaho Bureau of Mines and Geology, Bulletin 26, p. 23-42.

Lund, Karen, 1988, The Salmon River suture: An island arc-continent boundary, *in* Sharon E. Lewis and Richard B. Berg, ed., Precambrian and Mesozoic Plate Margins: Montana, Idaho and Wyoming with field guides for the 8th International Conference on Basement Tectonics: Montana Bureau of Mines and Geology, Special Publication 96, p. 103-110.

Lund, Karen, Derkey, P.D., and Oblad, Jon R., in prep., 1998, Digital geologic map of the Payette National Forest, and vicinity, Idaho: U.S. Geological Survey Administrative Report on CDROM

Lund, K., Alminas, H.V., Kleinkopf, M.D., Ehmann, W.J., and Bliss, J.D., 1990, Preliminary mineral assessment of the Elk City 1° x 2° quadrangle, Idaho and Montana: Compilation of geological, geochemical, geophysical, and mineral deposits information: U.S. Geological Survey Open-File Report 89-0016, 118 p.

Lund, Karen, Kunz, M.A., Manduca, C.A., Gammons, C.H., Evans, K.V., Tysdal, R.G., Winkler, G.R., and Connor, J.J., 1997, Geologic map of the western Salmon River Mountains, Valley and Idaho Counties, West-Central Idaho: U.S. Geological Survey Geologic Investigations Map 2599, scale 1:100,000.

Mabey, Don R., 1982, Gravity and magnetic features along the eastern margin of the Idaho batholith in central Idaho: Geological Society of America Abstracts with Programs v. 14, no. 6, p. 320.

Mabey, D.R., and Webring, M.W., 1985, Regional geophysical studies in the Challis quadrangle, *in* D.H. McIntyre, ed., Symposium on the geology and mineral deposits of the Challis quadrangle, Idaho: U.S. Geological Survey Bulletin 1658-E, p. 69-79.

Mabey, D.R., and Tschanz, C.M., 1986, Aeromagnetic survey and tentative interpretation, eastern part of the Sawtooth National Recreation Area, Idaho, Chapter B *in* Mineral Resources of the eastern part of the Sawtooth National Recreation Area, Custer and Blaine counties, Idaho: U.S. Geological Survey Bulletin 1545, p. 45-52.

Mabey, D.R., Zietz, Isidore, Eaton, G.P., and Kleinkopf, M.D., 1978, Regional magnetic patterns in part of the Cordillera in the western United States, *in* Cenozoic tectonic and regional geophysics of the western Cordillera: Geological Society of America Memoir 152, p. 993-106.

McCafferty, A.E., 1992, Magnetic maps and terrace magnetization maps for the Idaho Mineral Initiative Study, Idaho and vicinity: U.S. Geological Survey Geophysical Investigations Map, GP-994, scale 1:1,000,000.

Morelli, Carlo, Gantar, C., Honkasla, Tauno, McKonnel, R.K., Tanner, J.G., Szabo, Bela, Uotila, U.A., and Whalen, G.T., 1974, The international gravity standardization net 1972 (I.G.S.N.): Paris, Bureau Central de l'Association Internationale de Geodesie, Special Publication no. 4, 194 p.

O'Neill, J.M., and Lopez, D.A., 1985, Character and significance of the Great Falls tectonic zone, east-central Idaho and west-central Montana: American Association of Petroleum Geologists Bulletin, v. 69, p. 437-447.

Piccoli, P.M. and Hyndman, 1985, Magnetite/ilmenite boundary in the western Atlanta lobe of the Idaho batholith: northwest Geology, v.14, p. 1-5.

Pitkin, James A., in prep., 1998, Gamma-ray radioactivity of the Payette National Forest: U.S. Geological Survey

Plouff, Donald, 1977, Preliminary documentation for a Fortran program to compute gravity terrain corrections based on topography digitized on a geographic grid: U.S. Geological Survey Open-File Report 77-535, 43 p.

Prieto, Corine, Perkins, Carolyn, and Berkman, Ernst, 1985, Columbia river basalt plateau--An integrated approach to interpretation of basalt-covered areas: Geophysics, vol. 50, p. 2709-2719.

Schmidt, D.L., and Mackin, J.H., 1970, Quaternary geology of Long and Bear valleys, west-central Idaho: U.S. Geological Survey Bulletin 1311-A, 22 p.

Vallier, T.L. and Brooks, H.C., 1986, Paleozoic and Mesozoic faunas of the Blue Mountains province---A review of their geologic implications and comments on papers in the volume, *in* Vallier, T.L., and Brooks, H.C., eds., Geology of the Blue Mountains region of Oregon, Idaho and Washington---Geologic implications of Paleozoic and Mesozoic paleontology and biostratigraphy, Blue Mountains province, Oregon and Idaho: U.S. Geological Survey Professional Paper 1435, 196 p.

Watts, K.C. Jr. and King, Harley D., in prep., 1998, Geochemistry of the Payette National Forest: U.S. Geological Survey Open-File Report unpublished.

Yates, R.G., 1968, The Trans-Idaho discontinuity: Prague, Academia, XXIII Int. Geol. Congress, v. 1, p. 117-123.

Zietz, Isidore, Gilbert, F.P., and Kirby, J.R., 1978, Aeromagnetic map of Idaho--Color coded intensities: U.S. Geological Survey Geophysical Investigations Map GP-920.

Zietz, Isidore, Hearn, B.C., Jr., Higgins, M.W., Robinson, G.D., and Swanson, D.A., 1971, Interpretation of an aeromagnetic strip across the northwestern United States: Geological Society of America Bulletin, v. 82, no. 12, p. 3347-3372.

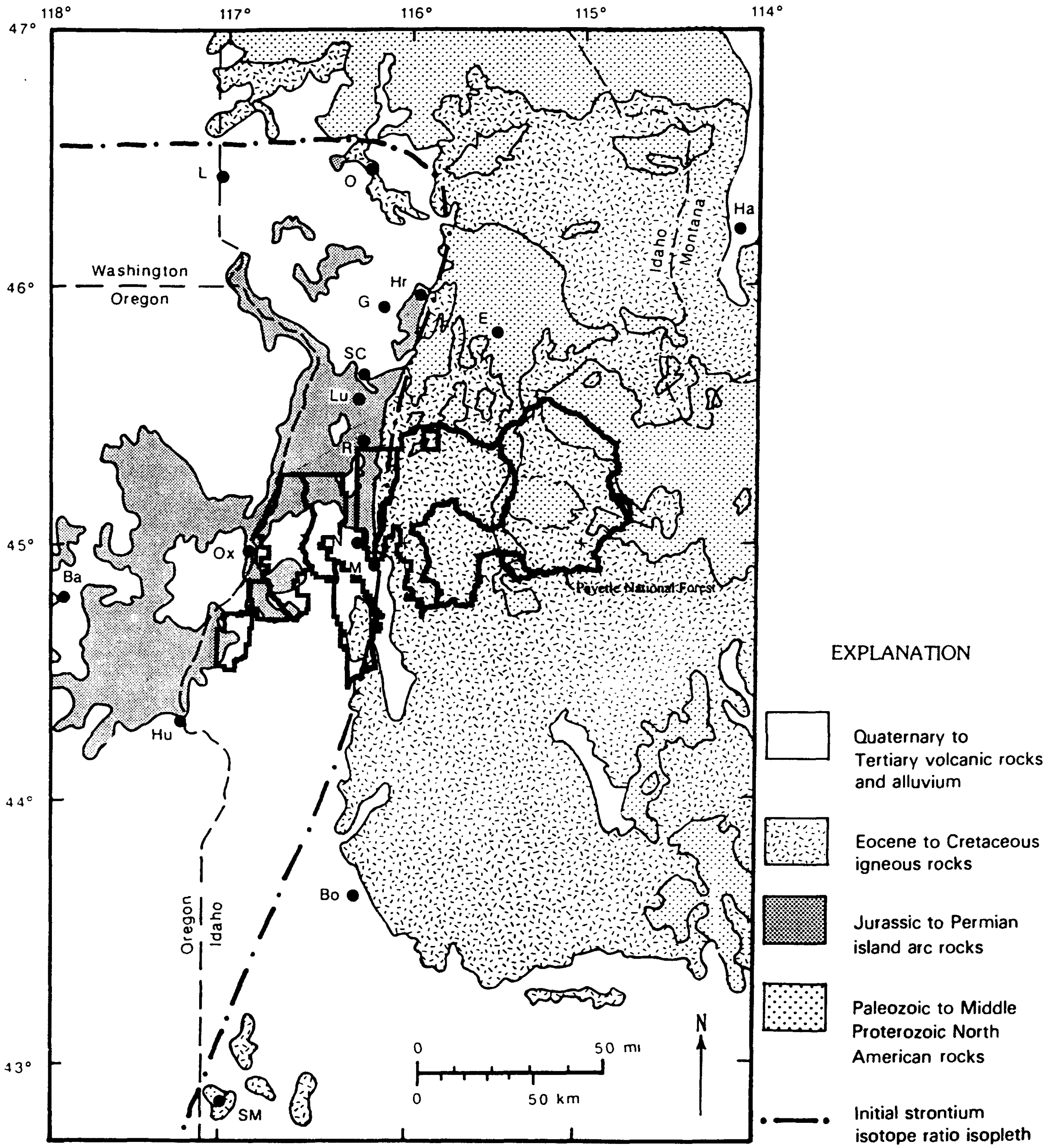


Figure 1 - Index map showing location of the Payette National Forest and generalized geology of west-central Idaho. Modified from Lund (1988 and 1997). Locations: Ba - Baker, BC - Big Creek, Bo - Boise, E - Elk City, G - Grangeville, Ha - Hamilton, Hr - Harpster, Hu - Huntington, L - Lewiston, Lu - Lucile, M - McCall, N- New Meadows, O - Orofino, Ox - Oxbow, R - Riggins, SC - State Creek, SM - South Mountain, YP - Yellow Pine. Initial strontium isotope line indicates oceanic values of $<0.704$ west of line and continental values of $>0.706$ east of line. This line represents the location of the Salmon River suture by showing the juxtaposition of basement blocks.

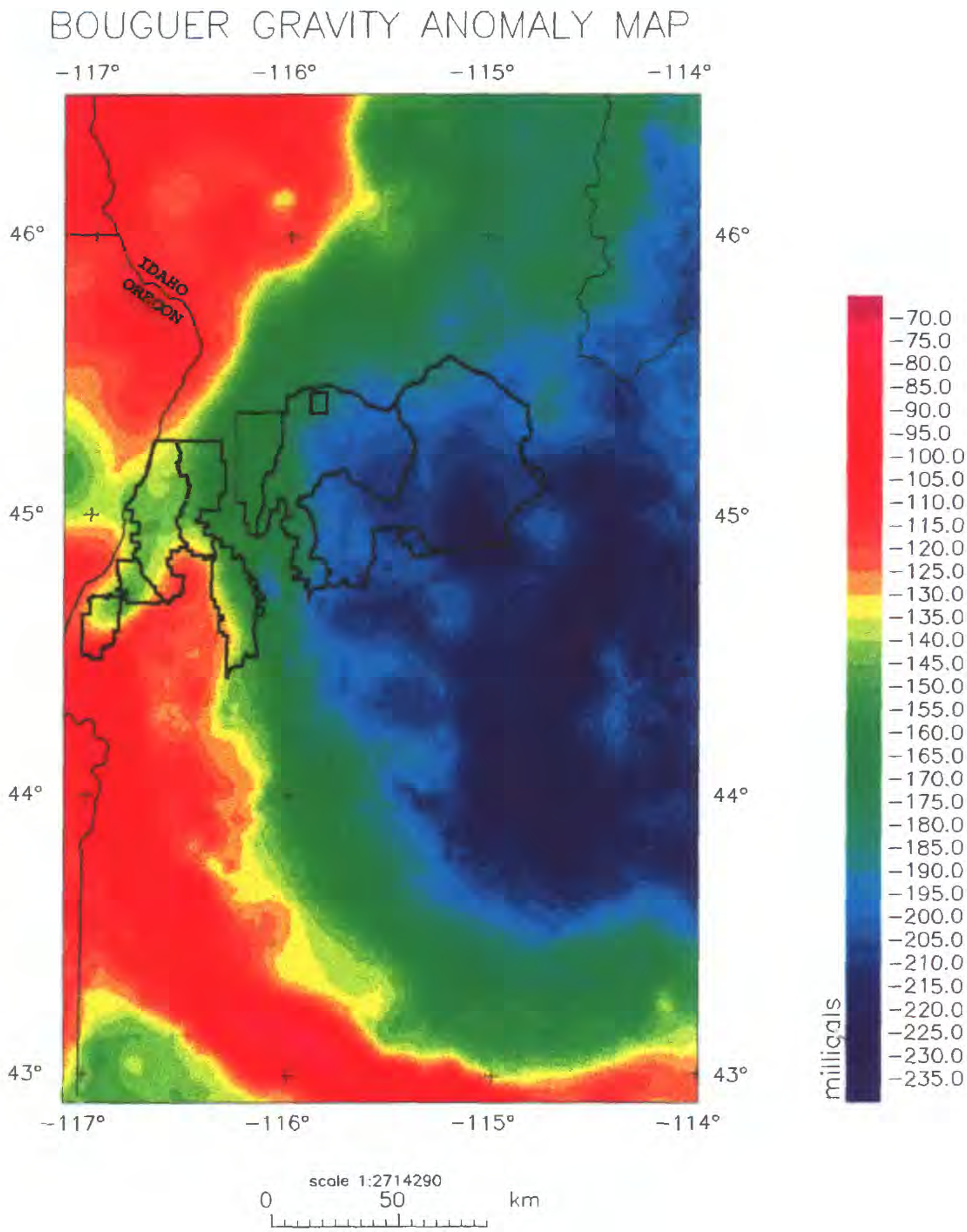


**Figure 2 - Bouguer gravity anomaly map of west-central Idaho showing boundary of Payette National Forest.**

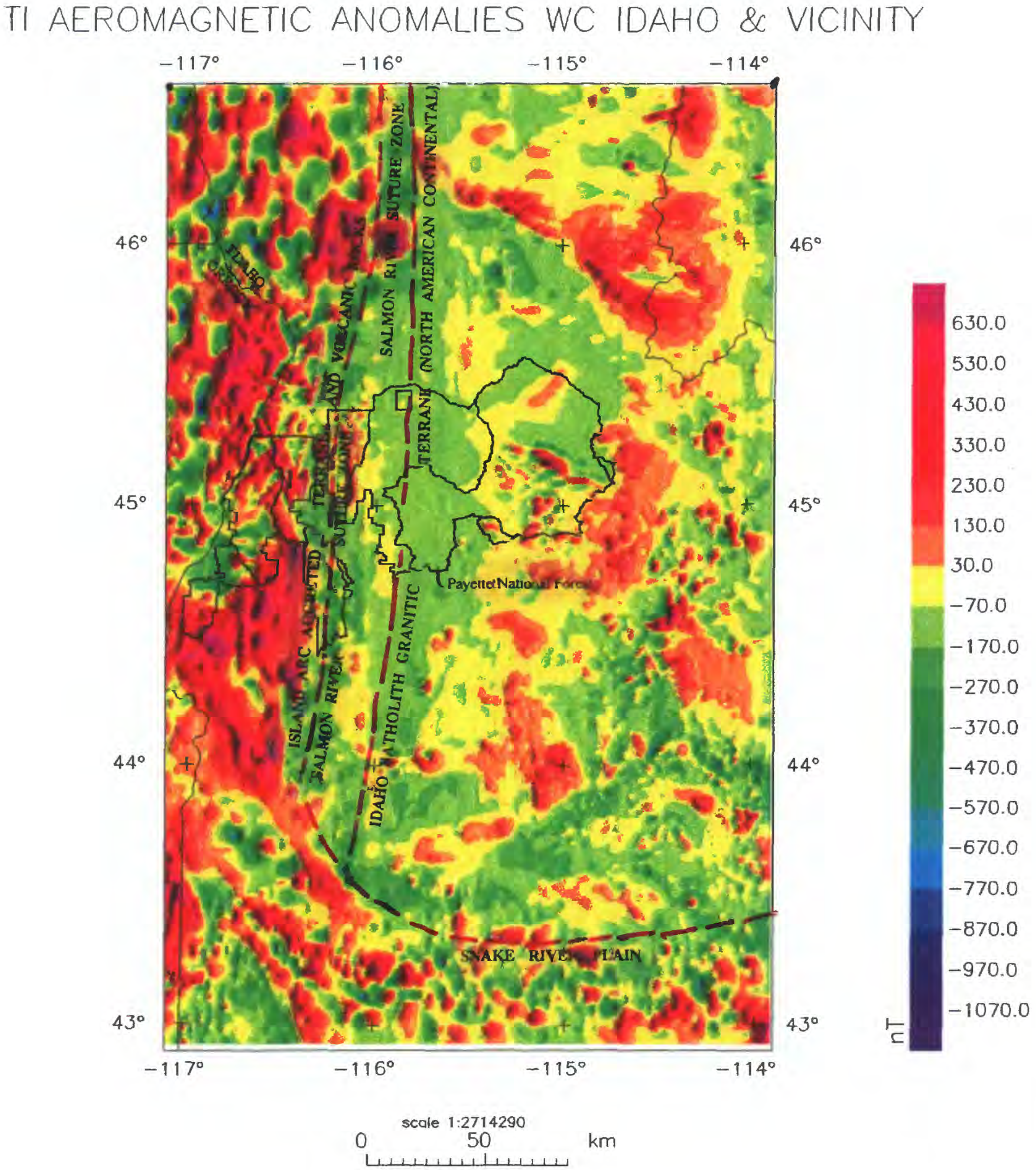


**Figure 3 - Total-intensity aeromagnetic anomaly map of west-central Idaho showing boundary of Payette National Forest and three geologic terranes - ISLAND ARC ACCRETED TERRANE, SALMON RIVER SUTURE ZONE TERRANE, and IDAHO BATHOLITH GRANITIC TERRANE (NORTH AMERICAN CONTINENTAL).**

# RESIDUAL AEROMAGNETIC ANOMALY MAP

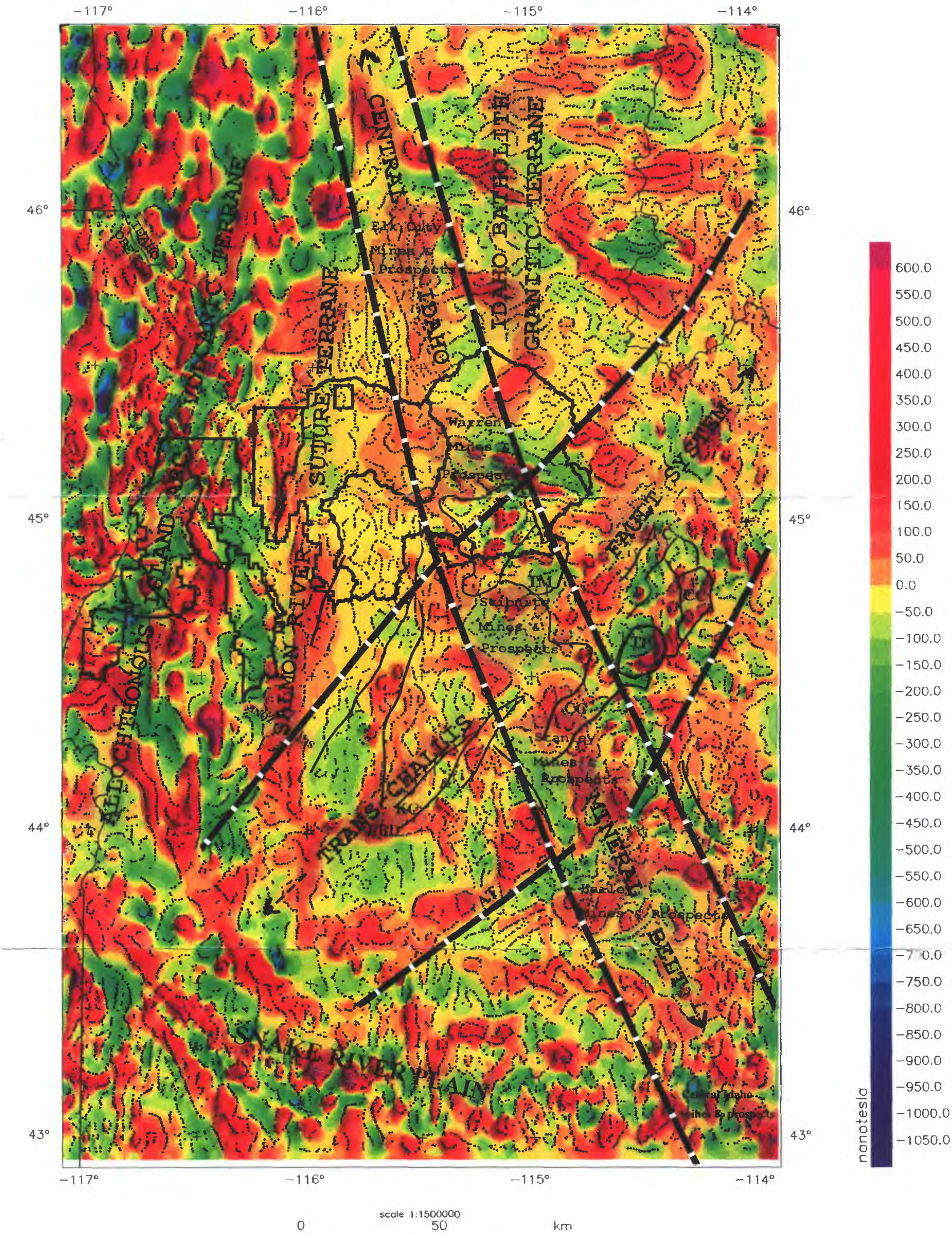


**Figure 4 - Residual aeromagnetic anomaly map of west-central Idaho showing major aeromagnetic anomaly trends based on high gradient zones of the pseudogravity (++++++), mineral belts, geologic terranes, and boundary of Payette National Forest . BBD - Boise Basin dike swarms CG - Custer graben KC - Knapp Creek graben PC - Panther Creek graben TM - Thunder Mountain caldera A - Atlanta shear zone TP - Twin Peaks caldera CC - Corral Creek cauldron.**

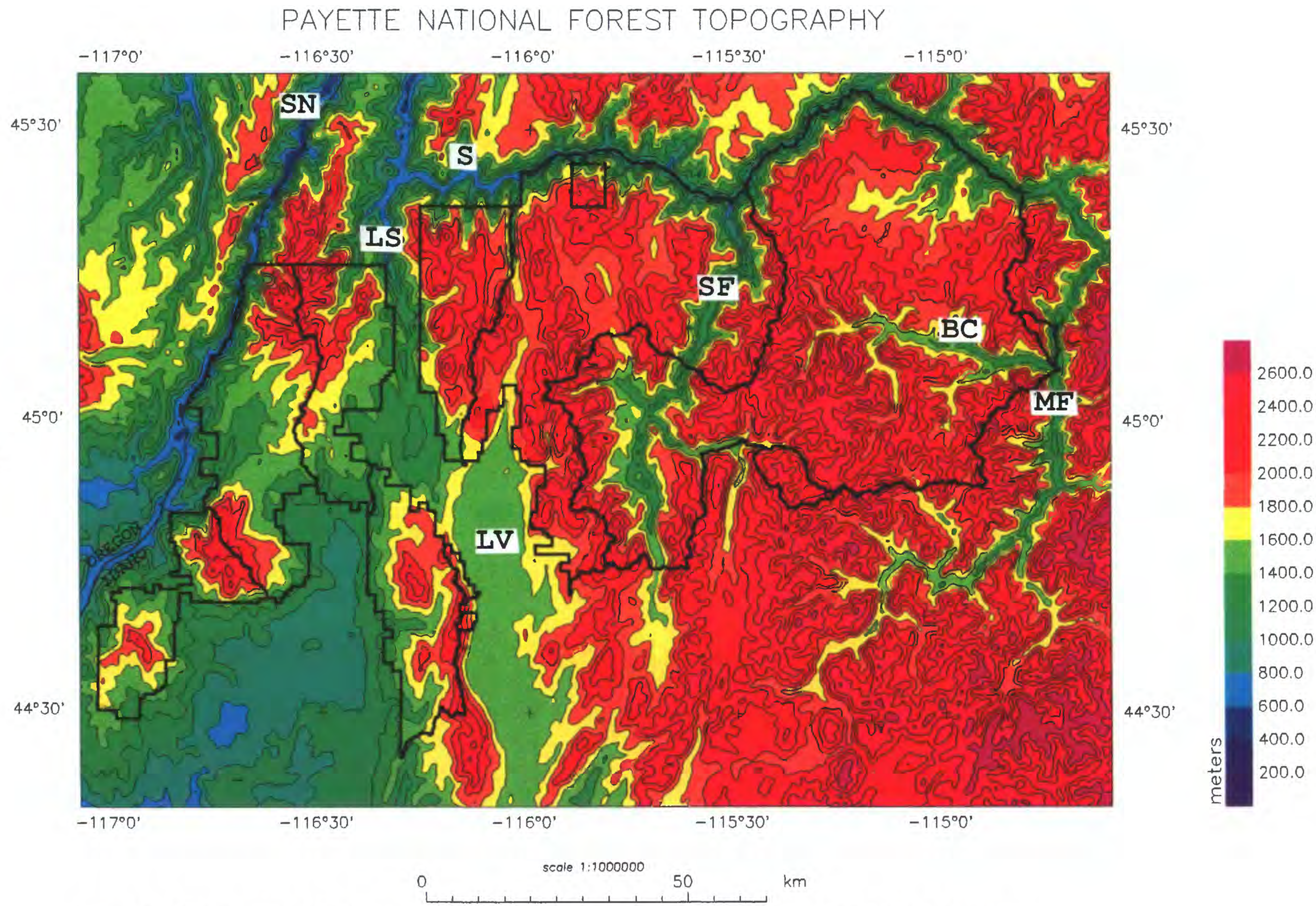


**Figure 5 - Elevation model of the study area showing boundary of Payette National Forest and major river drainages:**
**SN - Snake River (at Idaho-Oregon border), S - Salmon River, LS - Little Salmon River, SF - South Fork Salmon River, MF - Middle Fork Salmon River, BC - Big Creek ; LV - Long Valley.**

Map Units Modified from Generalized Geologic Map of Lund (Written commun., 1997)

- Q Quaternary alluvium and glacial deposits
- Tp Payette Formation sedimentary deposits
- Tw Basalt of Weiser
- Tcm Basalt of Cuddy Mountain
- Tcr Columbia River Basalt Group
- Tc Challis Volcanic Group
  Epizonal rhyolite to dacite dikes
- Tg Epizonal granite, granophyre, granodiorite, diorite and rhyolite/dacite
- Kg Biotite-muscovite granite and porphyritic muscovite-biotite granite/granodiorite
- Kgdf Foliated biotite granodiorite, hornblende-biotite tonalite
- Kgn Foliated/mylonized porphyritic granodiorite, hornblende tonalite, and metavolanic gneisses
- Kjqd Biotite-hornblende granodiorite-biotite quartz-diroite, gabbro
- I Izee terrane - greenstone volcanogenic fore-arc basin rocks
- O Olds Ferry terrane - greenstone metavolcanic and volcanogenic sedimentary island-arc rocks
- W Wallowa terrane - Quartz-dirotie, diorite, greenstone metavolcanic, carbonate rocks island-arc rocks; mafic gneiss rocks that are basement to Wallowa terrane. Includes wqd, w, wb of Lund (Written commun., 1997)
- TJ Medium- and high-grade metavolcanic, volcanogenic, and plutonic rocks. Includes $T_RJmv$ and $T_RJgn$ of Lund (Written commun., 1997).
- OZ Ordovician to Upper Proterozoic syenite and diorite complex
- P Metamorphized Paleozoic to Upper Proterzoic carbonate, shale, quartzite, quartite-pebble conglomerate, and volcanic miogeosynclinal rocks; metamorposed Paleozoic to Middle Proterozoic rocks, undifferentiated. Includes $P_ZZ$, $P_ZYq$, and $P_ZY$ of Lund (Written commun., 1997)
- Y Metamorphosed Middle Proteroziuc biotite phyllite, biotite-quartz phyllite, biotite gneiss, calc-silicate gneiss, quartz-rich gneiss, and miceous quartzite. Includes Yq, Yy, Ygn of Lund (Written commun., 1997)

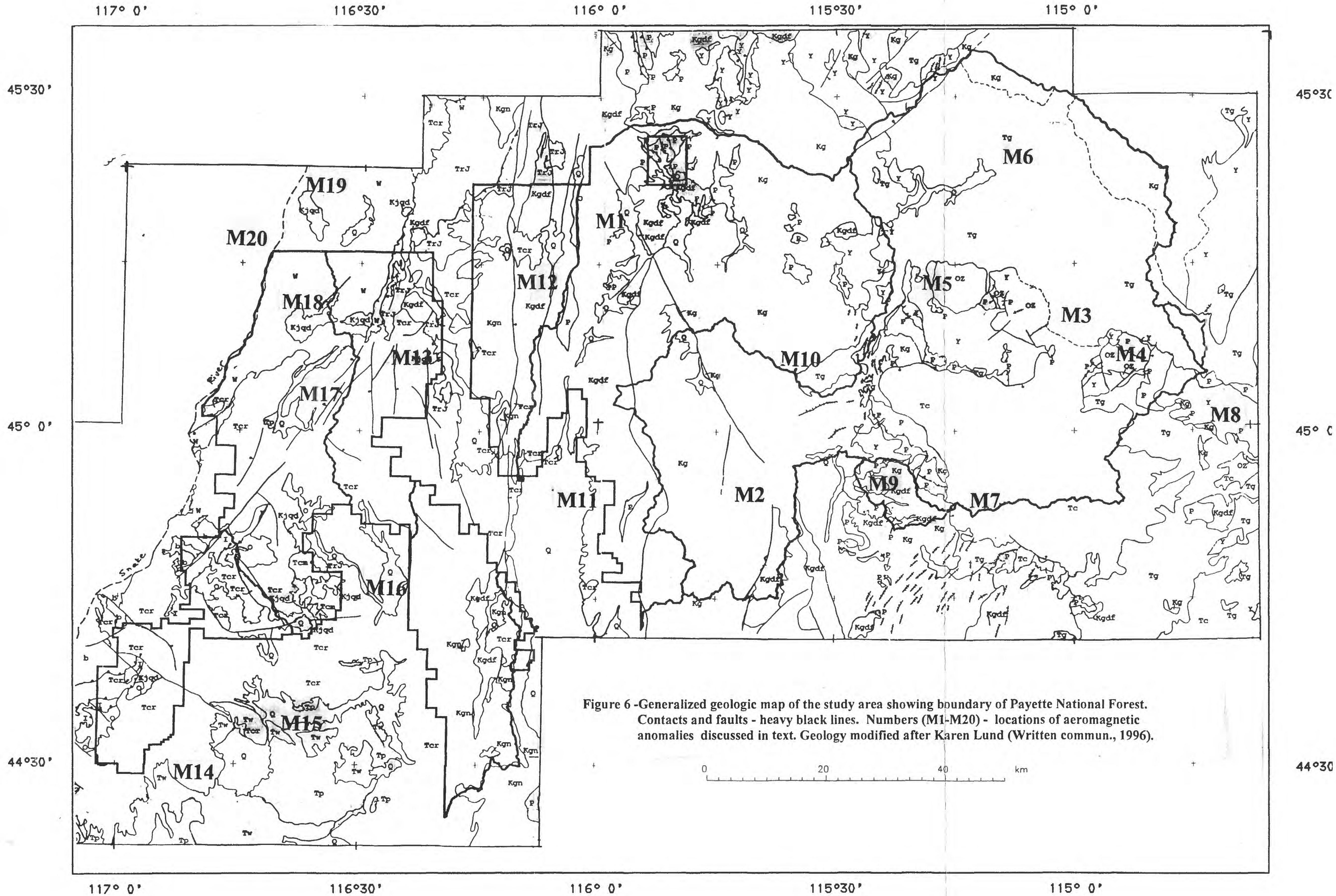


Figure 6 -Generalized geologic map of the study area showing boundary of Payette National Forest. Contacts and faults - heavy black lines. Numbers (M1-M20) - locations of aeromagnetic anomalies discussed in text. Geology modified after Karen Lund (Written commun., 1996).

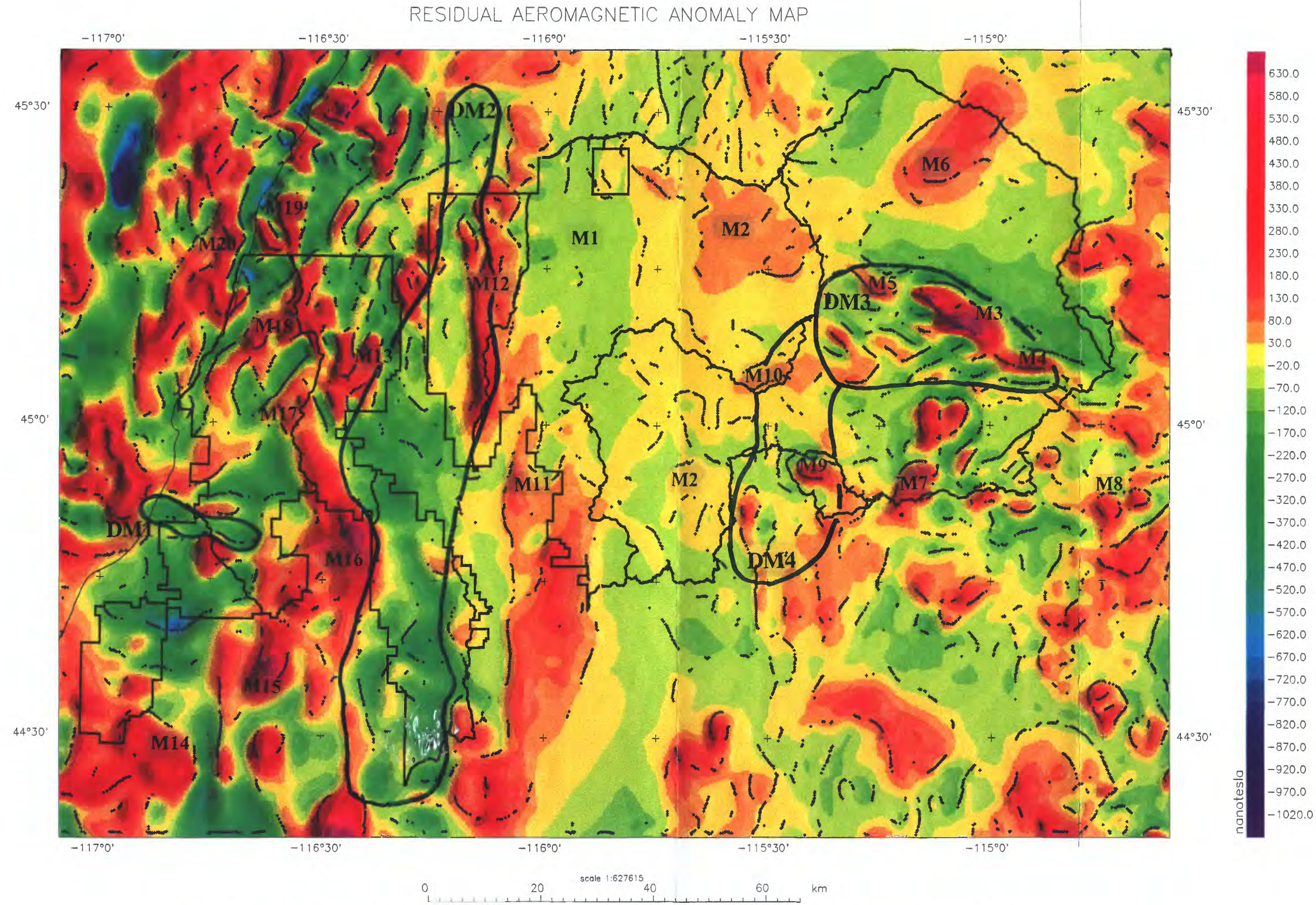


**Figure 7** - Residual aeromagnetic anomaly map of the study area showing trends of high gradient zones of the pseudo-gravity, permissive tracts for four mineral deposit models (DM1-DM4), and boundary of Payette National Forest. Numbers M1-M20 refer to anomalies discussed in text.

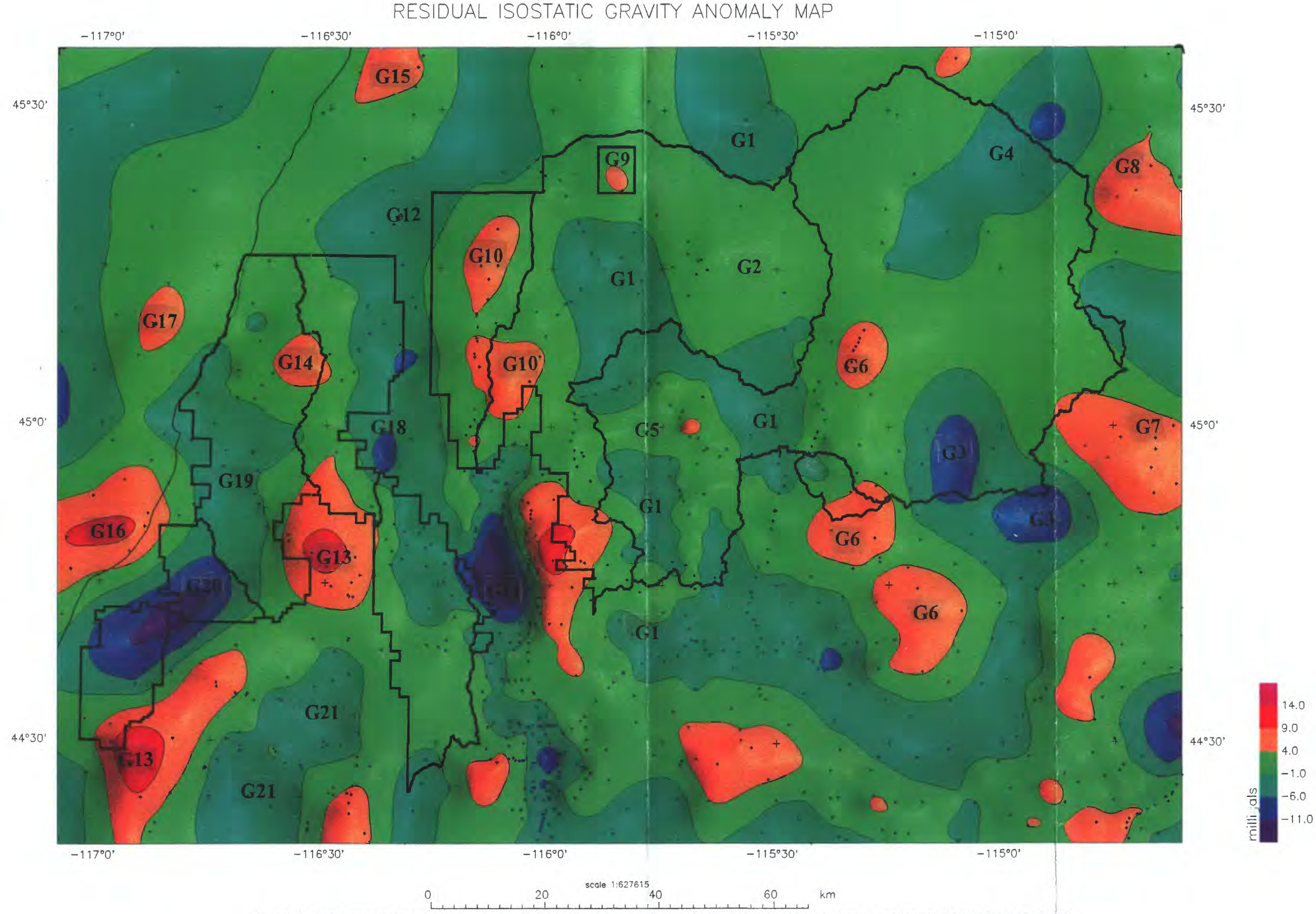


Figure 8 - Residual isostatic gravity anomaly map of the study area showing locations of gravity stations ( + ) and boundary of Payette National Forest. Numbers (G1-G21) refer to anomalies discussed in the text.